



CHORUS

This is the accepted manuscript made available via CHORUS. The article has been published as:

High-spin states and isomers in the one-proton-hole and three-neutron-hole ^{204}Tl isotope

R. Broda, K. H. Maier, B. Fornal, J. Wrzesiński, B. Szpak, M. P. Carpenter, R. V. F. Janssens, W. Królas, T. Pawłat, and S. Zhu

Phys. Rev. C **84**, 014330 — Published 26 July 2011

DOI: [10.1103/PhysRevC.84.014330](https://doi.org/10.1103/PhysRevC.84.014330)

High-spin states and isomers in the one proton- and three neutron-hole ^{204}Tl isotope

R. Broda,¹ K. H. Maier,¹ B. Fornal,¹ J. Wrzesiński,¹ B. Szpak,¹
M. P. Carpenter,² R. V. F. Janssens,² W. Królas,¹ T. Pawlat,¹ and S. Zhu²

¹*H. Niewodniczański Institute of Nuclear Physics PAN, PL-31342 Kraków, Poland*

²*Physics Division, Argonne National Laboratory, Argonne, IL 60439, USA*

(Dated: July 5, 2011)

The high-spin structure of the neutron-rich ^{204}Tl isotope has been studied up to a 11.2 MeV excitation energy and a $I = 30$ spin range using the deep-inelastic heavy-ion γ -spectroscopy method with reactions of ^{48}Ca on thick ^{208}Pb and ^{238}U targets. The established structure of yrast levels involves four isomeric states up to $I^\pi = 22^-$, the highest spin state available for the maximally-aligned four valence holes. The observations are interpreted and quantitatively confirmed by shell model calculations. The rates of the identified M2 and E3 isomeric decays are discussed and a striking analogy is found for the yrast level structures and γ decays observed in the 18^+ to 22^- and $45/2^-$ to $53/2^+$ spin ranges in ^{204}Tl and ^{203}Hg , respectively. In the highest spin part of the scheme two prominently populated yrast states are tentatively identified as the 3^- ^{208}Pb core excitation built on the 22^- and 20^+ maximally-aligned four-hole states. Their energies are reproduced well by using energy shifts observed in experiments for the ^{208}Pb core octupole excitation coupled to simpler intrinsic structures.

PACS numbers: 21.60.Cs, 23.20.Lv, 27.80.+w, 25.70.Lm

I. INTRODUCTION

Nuclei in the doubly-magic ^{208}Pb region provide one of the best playgrounds to test the accuracy with which the shell model can reproduce quantitatively experimentally established level structures [1, 2]. In this testing process, the set of shell model parameters has been constantly refined through the confrontation of calculations with new incoming experimental results and, presently, a valid description of many nuclei extends to high spin and excitation energy.

Recently, remarkable progress was achieved on the experimental side when deep-inelastic heavy-ion reactions started to be used for discrete γ spectroscopy [3]. This technique allowed to study the yrast structure in many nuclei in the vicinity of ^{208}Pb that were hitherto inaccessible for this kind of spectroscopic investigations, especially at the neutron-rich edge of the region (e.g. [4–6]). Moreover, in some of the already well-studied nuclei, the range of the observed excited states could be significantly extended to include yrast structures up to spin values of approx. $I = 30$ [3, 7]. The presence of many high-spin isomers is a favorable feature of nuclei in the Pb-region herewith simplifying spectroscopic studies. This fruitful line of experimental research activated new areas for verification of shell model calculations and posed challenges with the inclusion of more complex configurations that involve the core excitations required to form high-spin states. Specifically, the experimental study of the neutron-rich isotopes with $Z < 82$ provided (e.g. [8, 9]) an important input to constrain effective interactions involving proton holes used in calculations.

The $Z = 81$ one proton-hole neutron-rich Tl isotopes belong to the category of hard-to-reach nuclei and, until recently, the available experimental information on yrast levels was limited to a few selectively studied states

such as the long-lived 1.3 s, $11/2^-$ isomer in ^{207}Tl [10] or the 3.7 min, 12^- isomer in ^{206}Tl [11]. Noticeable progress was achieved already in early experiments using deep-inelastic reactions with heavy ions in which a few preliminary results on high-spin states were obtained [12, 13]. Later, the identification of isomers and higher-lying yrast levels in ^{205}Tl [14] displayed more extensively the potential of an experimental approach exploiting the appearance of isomers as the stepping stones from which the level structure can be expanded further. In the present work, we report results obtained in a full-scale study of high-spin states in the doubly-odd ^{204}Tl isotope where the coupling of three neutron- and one proton-holes gives rise to a sequence of isomeric states that can be understood well within shell model expectations. The present experimental results focus on isomeric states, but also include extended yrast structures located above the highest-spin isomer available for four valence holes. These obviously require that additional core excitations be considered.

The previous study of the ^{204}Tl nucleus assigned the 2^- spin-parity to the ground state and established a number of low-spin excited states populated in (n,γ) (d,p) (p,d) and (d,t) reactions [15]. Among those, the low-lying, $62 \mu\text{s}$, 7^+ isomer with a distinct yrast position and a configuration defined by a precise g -factor determination [16], is naturally expected to collect all the γ -decay intensity from higher-spin states. Recently, the existence of two higher-spin isomers decaying to the long-lived 7^+ state was reported within a much broader isomer search which used a ^{238}U fragmentation reaction [17]. The authors determined $2.6(2) \mu\text{s}$ and $1.6(2) \mu\text{s}$ half-lives, indicated the energies of several γ transitions from both isomeric decays and suggested 12^- and 20^+ isomer spin-parity assignments. These unambiguous identifications of γ transitions proved useful as a starting point for the

present analysis and are also consistent with the less certain isotopic assignment to ^{204}Tl derived from the cross-coincidence [3, 18] between transitions in the projectile-like and target-like fragments observed in deep inelastic data. Most recently, Fotiadis *et al.* [19] reported results of a ^{204}Tl study with the $(n,2n\gamma)$ reaction and gave results fully consistent with the present findings in the lower-spin part of the level scheme. In the next sections, a brief description of the experimental procedure, data analysis and results will be followed by a discussion of the observed levels with supportive guidance from shell model calculations.

II. EXPERIMENTAL PROCEDURE AND ANALYSIS

The γ coincidence data from a $^{48}\text{Ca} + ^{208}\text{Pb}$ experiment performed at the Argonne National Laboratory with the Gammasphere array, and used already in earlier spectroscopic analyses of other nuclei [6, 7], served to extract information on yrast levels in the ^{204}Tl isotope. In addition, the data from a similar experiment using the $^{48}\text{Ca} + ^{238}\text{U}$ system populating also ^{204}Tl with suitable yield were used to check some details of the level scheme and isomeric lifetime determinations. In both experiments, the ^{48}Ca beam from the ATLAS accelerator at ANL bombarded thick targets (50 mg/cm^2) of either ^{208}Pb or ^{238}U with a beam energy of 305 and 330 MeV, respectively. Targets were placed in the center of the Gammasphere array consisting of 101 Compton-suppressed HPGe detectors [20]. A pulsed beam was used with a 412 ns repetition time which enabled a clear separation of prompt and delayed events and provided a comfortable time range for new lifetime determinations. The γ rays emitted by the reaction products and detected in the Gammasphere detectors gave energy and timing signals that were indiscriminately collected in a standard set of coincidence events. The trigger condition required prompt coincidence of three γ rays and γ signals were stored within a 800 ns time range, following the trigger signal. For 12 hours, out of the 6-day experiment with the ^{238}U target, data were collected with a lower trigger requirement, allowing also 2-fold coincidences. This enabled the inclusion of low-multiplicity events arising from long-lived isomer and/or beta decays.

In the off-line analysis, the data were sorted in many ways using various time conditions which exploited isomeric lifetimes to achieve the best selectivity for various parts of the ^{204}Tl level scheme. Triple coincidences involving appropriate combinations of prompt and delayed γ rays served to produce clean coincidence matrices for required parts of the decay scheme by gating on intense lines above or below the isomer. Separate data sorts with the projection of the $T_{\gamma\gamma}$ parameter were performed for lifetime determinations. The γ energy calibration was precisely controlled by the known transitions from many well-studied nuclei produced in the same ex-

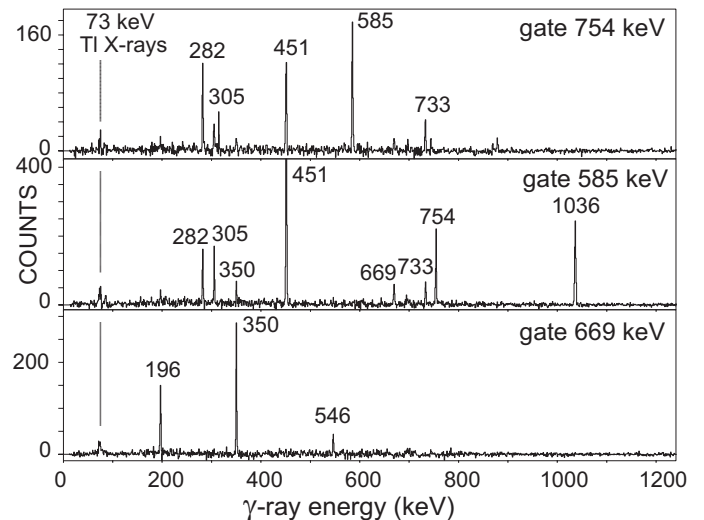


FIG. 1. Examples of γ coincidence spectra important to establish isomeric decays in ^{204}Tl below the 12^- (bottom panel) and the 18^+ isomers (two upper panels). See text for details.

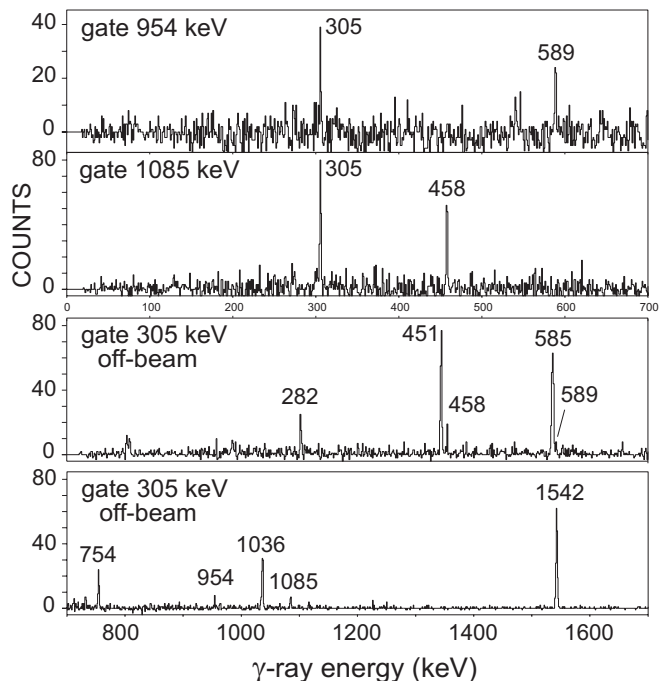


FIG. 2. The γ coincidence spectra selected to illustrate the decay of the 22^- isomeric state in ^{204}Tl . See text for details.

periment. Also, the detection efficiency, including the absorption in the target, was controlled by known low-energy transitions. Lifetime measurements were checked by inspection of events arising from decays of several well established isomers abundantly present in the data.

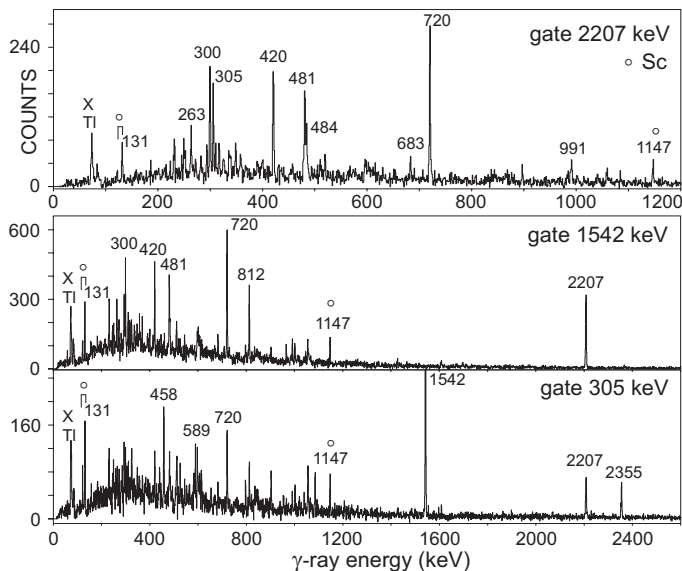


FIG. 3. The coincidence spectra of prompt γ transitions preceding in time the 18^+ and 22^- isomeric states in ^{204}Tl (see text for details). Lines marked by energies are identified as γ transitions located in the highest-spin part of the ^{204}Tl level scheme. Lines corresponding to $^{48,49}\text{Sc}$, which are in cross-coincidence with ^{204}Tl , are identified by open circles.

III. EXPERIMENTAL RESULTS

In the data from both the $^{48}\text{Ca} + ^{208}\text{Pb}$ and $^{48}\text{Ca} + ^{238}\text{U}$ experiments a satisfactory population of ^{204}Tl was recognized by the observation of coincidence events between the 414- and 690-keV γ transitions from the known $62 \mu\text{sec}$, 7^+ isomer decay. Transitions reported in the earlier identification of higher-lying isomers in ^{204}Tl [17] served to initiate the analysis, which revealed many new γ transitions belonging to the nucleus. By appropriate selection of time parameters and analysis of prompt and delayed coincidences, all γ transitions were readily sorted into families corresponding to deexcitations occurring between the isomeric states. Besides the two new isomers reported by Pfuetzner *et al.* [17], the presence of yet another higher-lying isomer was established together with extended sequences of prompt γ rays preceding in time all isomeric decays.

The list of all γ transitions identified in the ^{204}Tl nucleus is arranged in two separate tables. Table I gives energies as well as off-beam and in-beam intensities for all transitions occurring in isomeric decays, grouped in families corresponding to the γ decay of each isomer. For a number of low-energy transitions, the total electron conversion coefficient could be extracted with satisfactory accuracy from the decay intensity balance. These values are included in Table I and come from a quantitative analysis of various coincidence spectra; the resulting, mostly unique, multipolarity of several transitions is also indicated in the table. In Table II the energies, intensities and level scheme placements are listed for all prompt γ

transitions observed in ^{204}Tl . The vast majority belongs to a complex level structure observed above the highest-spin isomer, but as indicated, three transitions occur in the lower part of the level scheme. In later comments, we shall clarify the status of several transitions with energies below 400 keV which, at present, could not be safely placed in the level scheme.

Figures 1, 2 and 3 provide examples of coincidence spectra obtained with a selection of timing conditions and γ -energy gates appropriate to enhance the observation of the required parts of the level scheme. Figure 4 illustrates the isomeric decay patterns used to determine the half-lives of two isomers found in ^{204}Tl . The complete level scheme established in the present work from the detailed analysis of the coincidence data is displayed in Fig. 5.

TABLE I. Energies and relative intensities of γ transitions observed in isomeric decays identified in the ^{204}Tl isotope. Intensities of transitions below the 12^- isomer are normalized to the 669 keV (*) line intensity. Above the isomer, the strongest 585 keV (*) line intensity was used to normalize both, off-beam and in-beam intensities. Total electron conversion coefficients extracted from the intensity balance and resulting transition multipolarities are given in columns 4 and 5.

Transition energy E_γ (keV)	Relative intensity Off-beam I_γ	In-beam I_γ	Electron conversion α_{tot}	Init. level L^π	energy E_i (keV)
below 7^+	$62 \mu\text{s}$				1104.1
414.0 (1)	100*	–		E2	414.0
690.1 (1)	100*	–		E3	1104.1
below 12^-	$2.6 \mu\text{s}$				2319.0
196.2 (1)	33 (3)	–	1.30 (15)	M1	1650.1
349.8 (1)	62 (5)	–	0.33 (8)	M1	1453.9
546.1 (1)	21 (2)	–			1650.1
668.9 (1)	100*	–		E3	2319.0
below 18^+	420 ns				4391.6
282.1 (1)	15 (2)	10 (2)	0.6 (2)	M1	3637.3
451.0 (1)	77 (5)	62 (5)	0.11 (7)	(M1)	3355.2
585.2 (1)	100*	100*	0.1 (1)		2904.2
733.1 (1)	12 (1)	8 (3)			3637.3
754.3 (1)	35 (3)	17 (3)		(M2)	4391.6
1036.3 (1)	61 (4)	30 (5)		(E3)	4391.6
below 22^-	90 ns				6239.4
305.4 (1)	28.0 (20)	28.0*	0.18 (10)	E2	4697.0
457.6 (2)	4.4 (6)	3.0 (5)			5154.6
589.1 (2)	2.4 (4)	1.6 (3)			5286.1
762.7 (4)	1 (1)	–			5154.6
954.1 (3)	2.2 (5)	1.0 (4)			6239.4
1084.8 (2)	4.4 (8)	2.2 (4)			6239.4
1542.4 (1)	30.3 (20)	19.0 (15)		(M2)	6239.4

The bottom spectrum of Fig. 1 shows three γ lines coincident with the 669-keV isomeric transition from the

2319-keV isomer. In addition to the 669- and 350-keV transitions identified earlier [17] in the proposed 12^- isomer decay, we observed the new 196-keV transition coincident with the 350-keV line and the 546-keV cross-over transition which was mistakenly attributed earlier [17] to the higher-lying isomer. The long lifetime of the 7^+ isomer excluded the possibility to determine prompt intensities of higher-lying transitions from delayed coincidences with the 414- and 690-keV decay lines. However, the ordering of the 350- and 196-keV transitions present in the 2319-keV isomeric decay could be uniquely settled using the cross-coincidence technique. Prompt intensities of these lines, observed in coincidence with known γ rays of the corresponding Sc isotopes accompanying the ^{204}Tl isotope in the $^{48}\text{Ca} + ^{208}\text{Pb}$ reaction, clearly defined the ordering proposed in Fig. 5. This part of the level scheme is essentially consistent with the results of a recent spectroscopic study using the $(n,2n\gamma)$ reaction [19] which also placed the new 196-keV line, but mainly located a number of non-yrast, low-spin states not visible in the present study. The only apparent difference is the absence of a pair of 168- and 182-keV transitions that were placed in ref. [19] as competing with the 350-keV transition in the decay of the 1454-keV state. We could set an upper limit of 5% for the intensity of such a branch. As the timing conditions used in our experiments were not suitable to determine lifetimes in the microsecond range, we adopted in Fig. 5 a value of $61.7(10) \mu\text{s}$; i.e., the average from the Nuclear Data Sheets compilation [15] for the 7^+ level, and $2.6(2) \mu\text{s}$ from Ref. [17] for the 12^- isomer.

The next higher-lying isomer at 4392 keV did exhibit a more complex decay scheme involving three new transitions, besides the three most intense ones identified earlier [17]. Selected coincidences of γ rays preceding in time the 12^- isomer decay transitions, as well as delayed with respect to the most intense transitions above the 4392-keV isomer uniquely established the presence of the 282-, 451-, 585-, 733-, 754- and 1036-keV γ transitions between the isomers. The two upper spectra of Fig. 1 illustrate the quality of the data used to construct this part of the level scheme (Fig. 5). The unique ordering and placement of all transitions follows from the coincidence analysis and the prompt intensities listed in Table I. Except for levels populated in the isomeric decay, the presence of three prompt γ transitions of 489, 768 and 940 keV established two more levels at 3844 and 4612 keV that have no connection with higher-lying states. The determination of the 4392-keV isomer lifetime (see Fig. 4(a)) gave a much shorter half-life of $T_{1/2} = 420(30) \text{ ns}$ than the previously reported value $1.6(2) \mu\text{s}$ [17]. To justify better our result, in Fig. 4(c) we compare our half-life fit from Fig. 4(a) with the decay curves obtained for the known isomers of similar half-life range in ^{205}Pb [21] and ^{208}Pb [22]. The reason for this discrepancy is unknown since the presently established predominant feeding from the new, higher-lying isomer could not affect the previous determination due to its much shorter half-life, as will be shown below.

TABLE II. Energies and relative intensities of prompt γ transitions identified in the ^{204}Tl isotope. Initial level energies are given for transitions uniquely placed in the level scheme (see text for comments concerning unplaced transitions). Intensities are normalized to 28.0 units for the 305-keV transition intensity taken from Table I. Footnotes: a) transitions of prompt branches feeding the 3355.2- and 2904.2-keV levels, b) unresolved component observed in coincidence with the 720.2-keV transition.

Transition energy	Relative intensity	Initial level energy
E_γ (keV)	I_γ	E_i (keV)
182.4 (3)	0.42 (13)	7848.3
228.7 (3)	0.50 (15)	
231.3 (2)	1.46 (12)	
245.1 (3)	0.78 (16)	
249.3 (2)	1.07 (12)	
252.3 (3)	0.51 (4)	
263.2 (2)	1.22 (7)	9430.2
271.8 (3)	0.84 (19)	
293.7 (2)	2.09 (13)	
299.6 (1)	2.54 (8)	9167.0
305.4 (1)	28.0*	4697.0
309.8 (2)	1.15 (11)	
316.8 (2)	1.23 (15)	9483.8
336.2 (3)	0.77 (19)	
338.2 (3)	0.58 (17)	
343.5 (3)	0.19 (9)	
347.6 (3)	0.90 (15)	
357.4 (3)	0.83 (15)	
368.8 (3)	0.55 (18)	
390.7 (3)	0.83 (21)	
399.2 (3)	0.95 (18)	
420.6 (1)	2.93 (11)	8867.4
460.7 (3)	0.64 (15)	7665.9
480.7 (1)	3.47 (15)	9647.7
483.8 (2)	1.50 (15)	10905.1
489.5 (3) ^a	6.00 (80)	3844.2
519.3 (3)	0.45 (12)	10166.8
545.1 (3)	0.73 (17)	
683.0 (2)	0.95 (15)	10166.8
720.2 (1)	7.32 (25)	9167.0
720.0 (10) ^b	< 0.8	
768.2 (3) ^a	3.70 (50)	4612.2
796.9 (2)	1.60 (20)	7848.3
812.2 (1)	4.26 (21)	7051.5
902.8 (3)	1.80 (20)	9009.4
940.4 (4) ^a	4.50 (50)	3844.2
965.8 (3)	0.91 (12)	7205.2
983.7 (4)	0.45 (11)	9430.2
991.1 (2)	1.58 (12)	10421.3
1019.4 (4)	0.89 (25)	8867.4
1055.2 (2)	3.50 (20)	8106.6
1059.0 (5)	1.00 (25)	11225.8
1169.8 (5)	0.28 (14)	
1426.2 (4)	0.98 (15)	7665.8
1542.4 (1)	19.0 (15)	6239.4
2207.4 (1)	13.2 (11)	8446.8
2354.4 (2)	4.00 (23)	7051.5

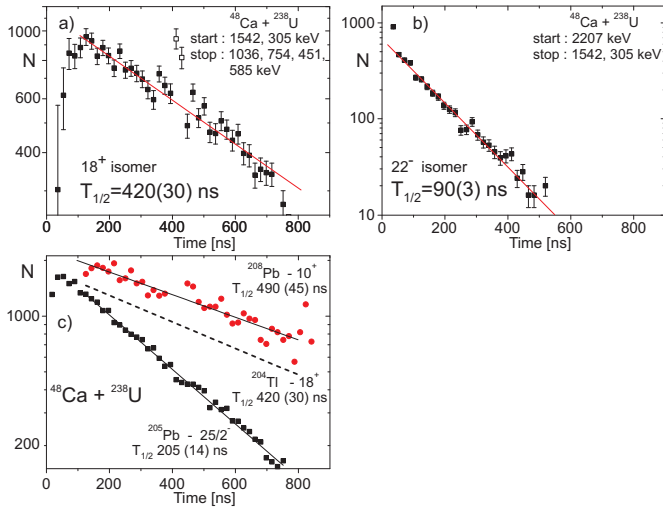


FIG. 4. Decay curves used for the half-life determination of the 18^+ (a) and 22^- (b) isomers in ^{204}Tl . Two points (open circles) involving random coincidences from γ rays associated with the next beam pulse were excluded from the fit. Fig. (c) shows decay curves obtained from the same $^{48}\text{Ca} + ^{208}\text{Pb}$ data for the well known isomers populated in ^{208}Pb (500(50) ns [22]) and ^{205}Pb (217(5) ns [21]). The dotted line shows fit from (a) for the 18^+ isomer decay in ^{204}Tl to justify the present half-life value lower by factor 4 than previously determined [17].

The coincidence spectra of Fig. 2 were selected to document the most important features of the decay of the new, highest-lying isomer located at an excitation energy of 6239 keV. Besides the weak 763-keV cross-over transition, all of the isomeric decay intensity proceeds via the most intense 305-keV yrast γ transition populated predominantly by the intense 1542-keV isomeric decay branch. The two bottom panels present the spectrum of γ rays coincident with the 305-keV gate and delayed with respect to the pre-selected most intense transitions above the isomer. Apart from transitions marked as occurring in the decay of the new isomer, the wide gate on the $T_{\gamma\gamma}$ parameter allowed to also observe transitions located below the 420 ns isomer, as well as traces of lines below the 2.6 μsec one. The two upper panels in Fig. 2 provide coincidences with the 954- and 1085-keV gates and document the presence of two other weak isomer-decay branches competing with the most intense 1542-keV transition. Fig. 4(b) shows the isomeric-decay curve used for the half-life determination of $T_{1/2} = 90(3)$ ns, as extracted from the $T_{\gamma\gamma}$ parameter with appropriate gates set on the strongest transitions below and above the isomer.

The coincidence spectra representative of the prompt transitions located in the highest part of the level scheme are displayed in Fig. 3.

One of the coincidence matrices was constructed for prompt transitions with the requirement that one of the strongest γ rays below 420 ns isomer is present in delayed coincidence. The bottom panel shows the spectrum ob-

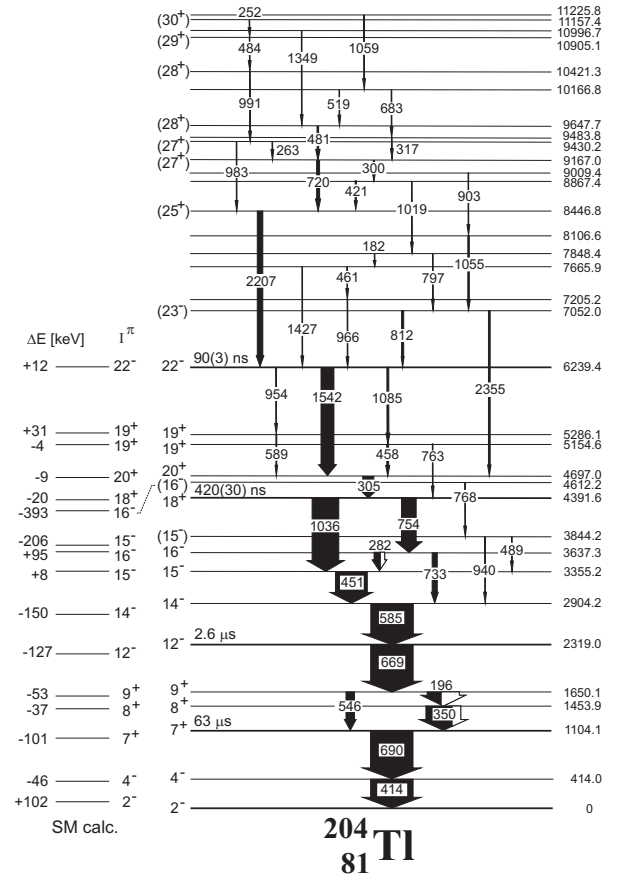


FIG. 5. The ^{204}Tl level scheme established in the present work. Shell-model calculated levels are shown to the left with ΔE (keV) values obtained as a difference between calculated and experimental binding energies relative to ^{208}Pb .

tained from this matrix with the gate set on the most intense 305-keV transition above the isomer, which deexcites the 4697-keV level. One observes a clear enhancement of prompt feeding and substantial reduction of coincidences with transitions preceding in time the 90 ns isomer. The observed intensity of the 458- and 589-keV transitions clearly locates them as the next higher-lying transitions determining the sequence in the 954-589 and 1085-458 keV cascades that is observed in the decay of the 90 ns isomer. This establishes two states at 5155 and 5286 keV. The high-energy 2355-keV transition seen in this spectrum apparently crosses the 90 ns isomer and feeds directly the 4697-keV state from the strongly populated yrast level located above the isomer. In all, in the spectra of Fig. 3, the presence of intense Tl X-ray lines and cross-coincidence γ rays from several known Sc isotopes reaffirm the association of the observed structure with the Tl isotope.

The medium panel of Fig. 3 displays γ rays preceding in time the 90 ns isomer. Here, the gate was set on the delayed 1542-keV isomeric transition with the precondition that one of the other intense lines below the 90 ns

or 420 ns isomers also appeared within the delayed time range.

Whereas only the most intense lines are marked by their energy, it is apparent that this spectrum is fairly complex, displaying many weaker γ transitions identified above the highest-lying isomer. They are listed in Table II. Finally, the high-statistics coincidence matrix of prompt γ transitions preceding the delayed γ rays from both 90 ns and 420 ns isomers was used to construct the level scheme above the highest-lying isomer. A coincidence spectrum for the high-energy 2207-keV gate, displayed in the upper panel of Fig. 3, demonstrates the quality of the data. The highest-spin and excitation-energy part of the level scheme established in this way (Fig. 5) includes only those transitions that could be uniquely placed on the basis of observed coincidence relationships and measured intensities. Many additional transitions listed in Table II were identified unambiguously as belonging to this high-spin part of the ^{204}Tl level scheme, but could not be placed with certainty. A notable feature was the presence of a series of low-energy transitions in cascades that could not be placed due to their complex connection to known, lower-lying levels. We may only indicate two such cascades of 294-231-348-390 keV and 310-249-294-357-399-457 keV transitions that show clear mutual coincidence relations, but could not be located in the level scheme.

In the following section, we shall discuss spin-parity assignments and the interpretation of states located below the highest-lying isomer. Only selected aspects concerning higher-lying states that extend to a 11.2 MeV excitation energy and a spin close to $I = 30$ will also be addressed.

IV. SPIN-PARITY ASSIGNMENTS, CALCULATIONS AND DISCUSSION

A. Structure of isomeric states

The sequence of ^{204}Tl energy levels established in this work up to the highest-spin 22^- isomeric state at 6239 keV can be understood well by considering simple shell model configurations involving four valence holes. In particular, the firmly established four isomeric states can be naturally interpreted as arising from the energy-favored couplings of one-proton and three-neutron holes to high-spin states located at distinct yrast positions. The single-particle states $p_{1/2}$, $f_{5/2}$, $p_{3/2}$, and $i_{13/2}$ are available for the three neutron holes below the $N = 126$ gap, and the one proton hole must occupy one of the $s_{1/2}$, $d_{3/2}$, or $h_{11/2}$ states located below the $Z = 82$ gap. It is clear that, from those single-particle states, the high- j neutron $i_{13/2}$ and proton $h_{11/2}$ orbitals will feature prominently in the structure of isomeric states. The next, more tightly bound orbitals, $f_{7/2}$, $h_{9/2}$ for neutrons and $d_{5/2}$, $g_{7/2}$ for protons, are energetically unfavorable to gain spin. However, as will be discussed later, they

were included in the calculations and were found to be important to explain the observed M2- and E3-transition rates.

The structure of the lowest-lying, 7^+ isomer was established earlier (with support of a precise g -factor measurement [16]) as a mixed state with a predominant $\pi s_{1/2}^{-1}\nu i_{13/2}^{-1}(\nu^{-2})_0$ configuration. The spin-parity assignment and interpretation of the 12^- isomer at 2319 keV is also straightforward as arising from the $\pi h_{11/2}^{-1}\nu i_{13/2}^{-1}(\nu^{-2})_0$ coupling, which is the highest-spin state available when the two remaining neutron holes are paired to spin 0. Such a 12^- isomer is known in ^{206}Tl at 2643 keV [11], although the M4 transition (being in this case the only possible γ decay) results in the very long ($T_{1/2} = 3.7$ min) half-life of this state.

At the other extreme, the excitation energy and the expected spin range of the highest-lying isomer at 6239 keV strongly suggest the 22^- assignment expected for the coupling to maximum spin of three $i_{13/2}$ -neutron holes with a $h_{11/2}$ -proton hole. The observed structure of yrast levels above this isomer and, specifically, the high energy of the most intense yrast 2207-keV transition clearly suggest that the spin of this isomeric state exhausts the maximum value available for four valence holes and that, subsequently, core excitations are required to produce any higher spin excitation. Consequently, the intermediate isomer at 4392 keV can naturally be assigned as the 18^+ state with a $\pi h_{11/2}^{-1}\nu i_{13/2}^{-2}p_{1/2}^{-1}$ predominant configuration in which one neutron hole remains in the lowest-energy $p_{1/2}$ orbital.

With these initial considerations in mind, we have performed shell-model calculations to obtain a complete set of states while confirming suggested spin-parity assignments for the four isomeric states. These assignments then served in turn as benchmarks for the spin-parity assignments and the interpretation of all other levels observed in the isomeric decays.

B. Shell-model calculations

The OXBASH shell-model computer code [23] was used to calculate energy levels in the ^{204}Tl nucleus. The full configuration space, extending between ^{132}Sn and ^{208}Pb , was adopted without restriction, using single-particle energies derived from the latest experimental excitation energies of the appropriate states in one-hole nuclei and from the 2003 mass evaluation tables [24]. The starting point for selection of the final set of two-body matrix elements (TBME) was the p-n and p-p interaction of Rydström *et al.* [1] and the n-n interaction of McGrory and Kuo [25]. These interactions have then been adjusted and complemented by considering revised single-proton energies and energies of recently located states, particularly of high-spin states involving $h_{11/2}$ protons and $i_{13/2}$ neutrons. The detailed description of all these modifications and the discussion of the experimental results that were used to adjust the two-body matrix elements are

given in a paper devoted to our most recent study of high-spin states in ^{203}Hg [26]. Here, we shall only emphasize the conclusion that, with these modifications, a significantly improved agreement was obtained between the calculated and experimental energies of excited states in Pb, Tl and Hg isotopes with mass numbers 205 and 204. Whereas the experimental energy of the presently established 22^- isomer in ^{204}Tl was also used to extract one corresponding TBME, the excellent agreement between new experimental and calculated levels in ^{203}Hg , with a mean quadratic error of only 103 keV, gave confidence in the obtained shell-model results. Nevertheless, in a full comparison of all calculated and experimental states, one should be aware of restrictions related to the fact that only a small fraction of the diagonal matrix elements could be adjusted to known states and, moreover, that there is hardly any knowledge about mixing matrix elements from experiment.

The results of the ^{204}Tl calculations are displayed in Fig. 6, where the two lowest-energy calculated states are indicated for both positive and negative parity at each spin value up to $I = 22$. A characteristic general feature of the calculations is the distinct interchange in yrast status of sequences of positive- and negative-parity states in subsequent spin ranges. The observed energy separation of different parity states is so pronounced that, within the expected accuracy of the calculations, the parity assignments for states established in the experiment can be proposed with confidence. In particular, the distinct yrast position of four states at $I^\pi = 7^+$, 12^- , 18^+ and 22^- observed in Fig. 6 fully confirms the anticipated spin and parity of the four experimentally-established isomeric states with the main configuration discussed above. The structure of the 22^- state is of pure $\pi h_{11/2}^{-1}\nu i_{13/2}^{-3}$ character and the calculated wave functions indicate 72% of the $\pi h_{11/2}^{-1}\nu i_{13/2}^{-2}p_{1/2}^{-1}$ configuration as the predominant structure of the 18^+ isomeric state. For the 12^- isomer, the $\pi h_{11/2}^{-1}\nu i_{13/2}^{-1}(\nu^{-2})_0$ configuration exhausts 71% of the state structure when all contributions from neutron pairs distributed in the $p_{1/2}$, $f_{5/2}$ and $p_{3/2}$ orbitals are included. The lowest 7^+ isomer and the 2^- ground state are more complex. Whereas the summed amplitudes of the $\pi s_{1/2}^{-1}\nu i_{13/2}^{-1}(\nu^{-2})_0$ configurations amount to 50% of the 7^+ isomer structure, the ground state is most strongly mixed with the largest contribution of 32% assigned to the $\pi s_{1/2}^{-1}\nu p_{1/2}^{-2}f_{5/2}^{-1}$ configuration. In general, the discussed structures and calculated results clearly indicate that all of the identified isomeric decays must involve parity changing transitions. For these four isomers, the agreement between the calculated and experimental binding energies relative to ^{208}Pb is excellent, with $E_{cal} - E_{exp} = -101, -127, -20, \text{ and } +12$ keV for the $I^\pi = 7^+, 12^-, 18^+, \text{ and } 22^-$ states, respectively. As a result, these spin-parity assignments to the four isomers can be considered firm and they become the basis for the assignments of all other levels located between them.

A full comparison of the calculated and experimen-

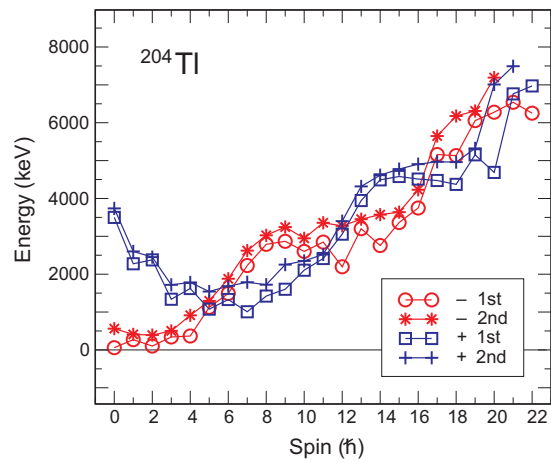


FIG. 6. Calculated shell-model levels for ^{204}Tl . For each spin, the two lowest energy states are shown for negative and positive parity as indicated in the legend.

tal levels is displayed with the level scheme of Fig. 5, where among all the calculated levels only those matching clearly their experimental counterparts have been selected.

It has to be noted that the theoretical energies are not presented in the usual way as calculated excitation energies above the ground state. Instead, in Fig. 5, a more meaningful presentation was adopted showing, for each level, the difference between the calculated and experimental binding energies. For ^{204}Tl , the binding energy of the 2^- groundstate relative to ^{208}Pb is known with high precision as 28905(2) keV from the measured mass excesses [24]. The calculations determine this binding as 29007 keV, an agreement at the 0.3% level, which is notable in view of the highly-mixed nature of the groundstate configuration. The resulting difference 29007 - 28905 = +102 keV of Fig. 5 indicates that the calculated groundstate is not sufficiently bound. It is clear from the corresponding differences (see Fig. 5) that, for the states of highest spins with rather pure wave functions, the agreement improves by about a factor of 10.

The mean linear difference between calculated and measured binding energies of the 14 yrast levels is -21 keV and the mean quadratic deviation is 72 keV. Although this article focusses on high-spin states, it may be pointed out that a few levels with spin 3 or less are known below 425 keV [15, 19]. The calculations also show several low-spin states of negative parity in this energy range. This agreement emphasizes the reliability of the shell-model calculations and confirms the proposed spin-parity assignments.

C. Spin-parity assignments and level interpretation for states located between isomers

In the following, we discuss spin-parity assignments to all levels populated in the subsequent isomeric decays

shown in the level scheme of Fig. 5. Along with the guidance from calculations, we used experimental input by taking into account the observed γ decays, yrast population arguments and the multipolarities of some low-energy transitions obtained from the extracted total conversion coefficients.

The 2^- and 7^+ assignments to the ground state and the lowest-lying isomer, together with an isomeric half-life strongly favoring an E3 character for the 690-keV isomeric transition, settle the 4^- spin-parity for the intermediate level at 414 keV. This firm assignment was also made by the NDS evaluators [15] based on the (d,α) [27] and (p,d) [28] reaction data, although a shifted level energy of 428(2) keV was taken from Ref. [28]. The calculated energy of the lowest 4^- state agrees well with the experimental value and the next calculated 4^- state is much too high in energy (957 keV) to be populated in the 7^+ isomer decay with any detectable intensity.

The established M1 character of the 196- and 350-keV transitions (see Table I) and the E3 character of the isomeric 669-keV transition (see above), result in an unambiguous assignment to the 1454-keV 8^+ and 1650-keV 9^+ states populated in the 12^- isomer decay. Both experimental level energies agree well with the calculated 8^+ and 9^+ levels and the intensity of the observed 546-keV transition is adequate for an E2 cross-over branch competing with the 196-keV M1 transition.

In a more complex part of the level scheme, between the 12^- and 18^+ isomers, three states are populated reflecting the yrast decay that can be expected for the calculated sequence of states (Fig. 6). Guided by the close agreement of the calculated and experimental energies, we assign the 2904-, 3355- and 3637-keV states as $I^\pi = 14^-, 15^-$ and 16^- , respectively. The observed γ decay strongly favors these assignments with such important considerations as the established M1 character of the 282-keV, $16^- \rightarrow 15^-$ transition, a strongly-preferred M1 character for the 451-keV transition, the presence of the competing 733-keV line, proposed as the $16^- \rightarrow 14^-$ E2 cross-over, and the clear absence of a cross-over transition from the 3355-keV level to the 12^- isomer. Consequently, the 1036- and 754-keV isomeric transitions represent the competing E3 and M2 branches for which the reduced transition probabilities will be discussed below.

In this part of the level scheme, two other levels, located at 3844 and 4612 keV, are not populated in isomeric decays, but are firmly established as non-yrast states with most likely 15^- and 16^- respective assignments. This choice is made based on the observed γ decays and on calculation results (Fig. 6), although in both cases the energies of the experimental states are significantly higher than their calculated counterparts. The 3844-keV experimental level energy is higher by 163 keV than the calculated second 15^- state and the 4612-keV, 16^- candidate is shifted upwards by more than 300 keV compared to the energy of two close-lying 16^- non-yrast calculated states. In any case, the inspection of calculated levels hardly allows to consider any other assign-

ment and the observed deviation of the energies can be attributed to the poorly known off-diagonal matrix elements in the shell-model calculations. Apparently, a mixing of the considered states is more effective in pushing the non-yrast partner levels to higher energies. It can be noted that the experimental energies of both the 15^- and 16^- yrast states, in particular that of the latter level, are lower than the calculated yrast levels. This may also result from the suggested mixing.

The very intense 305-keV E2 transition above the 18^+ isomer establishes the uniquely assigned $I^\pi = 20^+$ state located at the distinct yrast position (Fig. 6) of 4697 keV, in close agreement with the calculated energy for such a 20^+ level. Among the calculated levels in this excitation energy range, below the 6239-keV 22^- isomer, there are no other states with spin $I = 20$ or higher. However, one finds two 19^+ levels calculated at energies very close to the excitation energy of two experimental states located at 5155 and 5286 keV and populated by direct branches from the 22^- isomeric state. The observed γ decay of both states is consistent with such a 19^+ assignment. In particular, the existence of a weak competing M1 branch of 763 keV, which feeds directly the 18^+ isomer from the lower-lying 5155-keV level, could be established due to the stronger population of this state. Thus, for both experimental states, the 19^+ assignment was adopted and, consequently, the corresponding transitions feeding both states were characterized as E3 branches competing with the predominant 1542-keV M2 decay of the 22^- isomer. The review of all observed E3 and M2 decays of the ^{204}Tl isomers will be discussed in the next subsection along with a noteworthy analogy with the recently studied ^{203}Hg nucleus [26].

The detailed discussion of the ^{204}Tl states located between the isomers would require an extensive presentation of their wave functions which often exhibit a fairly complex intrinsic structure involving a number of configurations. Here, we restrict ourselves to a general feature that applies to the level scheme: each of the isomers feeds a sequence of states with the same parity. This arises from the coupling of the remaining available neutron holes which are all located in orbitals with the same, negative parity; i.e. the $p_{1/2}$, $f_{5/2}$ and $p_{3/2}$ states. Thus, above the ground state and the two lowest-lying isomers, which both involve a single $i_{13/2}$ neutron hole, the higher-lying states arise from breaking one additional pair of neutron holes and coupling them appropriately in order to gain the spin available from the three orbitals. Apparently, the mixed 2^+ coupling of the two neutron holes is favored as the $\Delta I = 2$ excitations are featured strongly in the lowest yrast excitations located above the isomers (see the 414-keV, $4^- \rightarrow 2^-$, the 546-keV $9^+ \rightarrow 7^+$, and the 585-keV $14^- \rightarrow 12^-$ transitions).

In the case of the 18^+ isomer, the situation is even simpler as the state's structure involves two $i_{13/2}$ neutron holes and only a single additional neutron hole is available. Here, starting from the structure discussed earlier with a main (72%) $\pi h_{11/2}^{-1} \nu i_{13/2}^{-2} p_{1/2}^{-1}$ configuration, a sim-

ple promotion of the $p_{1/2}$ neutron hole to the empty $f_{5/2}$ state explains the 305-keV E2 excitation above the isomer. Consequently, the structure of the 20^+ state has a predominant $\pi h_{11/2}^{-1} \nu i_{13/2}^{-2} f_{5/2}^{-1}$ amplitude. Indeed, the calculated wave function involves this configuration as a 98% component, making the 20^+ state the second one with the purest intrinsic structure, after the 22^- isomer.

D. Reduced E3 and M2 transition probabilities and analogy with ^{203}Hg

As pointed out above, all of the isomeric states established in the ^{204}Tl isotope decay by parity-changing E3 or M2 isomeric transitions. Table III presents a compilation of reduced transition probabilities extracted from the measured half-lives and branching ratios for the five E3 and two M2 transitions observed in the ^{204}Tl isomeric decays. For comparison, Table III includes corresponding values obtained for E3 and M2 transitions observed in the known ^{205}Tl [14] and ^{203}Hg [26] isomeric decays. In general, one notices that the experimental values of the transition probabilities for all E3 transitions are within a factor of 10 of each other in a range close to the single-particle unit, and that all the M2 transitions are strongly retarded, by a factor 10^{-3} , compared to the Weisskopf estimates. The main single-particle hole states involved in the structure of the corresponding states define both E3 and M2 transitions as strictly forbidden, since for both neutrons and protons $\Delta j = 4$ is the smallest change in the spin value between different parity orbitals. Thus, it is evident that to proceed, both E3 and M2 transitions must use small wave function amplitudes involving deeper bound states. The next available ones, i.e., the $f_{7/2}$ neutrons and $d_{5/2}$ protons, are good candidates to contribute with favorable $\nu i_{13/2} \rightarrow f_{7/2}$ and $\pi h_{11/2} \rightarrow d_{5/2}$ E3 transitions; their strength is about 24 W.u. due to strong mixing with the collective octupole excitation in ^{208}Pb . Inspection of the calculated wave functions indicates admixtures of these orbitals of the order of 1%. Taken together, this explains the observed transition probabilities of the order of 1 W.u. The variation between 0.1 and 3 W.u. is understandable as several components of the wave functions contribute to various degrees and may interfere in a constructive or destructive way. Incidentally, the $25/2^+$ isomer of ^{205}Tl , which involves a similar 12^- structure coupled to a $p_{1/2}$ neutron-hole also decays by a relatively fast E3 transition of 1.5 W.u., as does the 12^- level with 3 W.u. The observed stability of the reduced transition probabilities for other E3 transitions established in the ^{204}Tl and ^{205}Tl nuclei is noteworthy, as all of the values are rather close to 0.5 W.u. Also, all of the observed M2 transition probabilities display a remarkable stability with values similar to within a factor 4 and with the same retardation factor of 10^{-3} compared to single-particle estimates. The only possibilities for M2 transitions involve $\nu i_{13/2} \rightarrow h_{9/2}$ and $\pi h_{11/2} \rightarrow g_{7/2}$ changes in orbital occupancies. The

deeply bound $\nu h_{9/2}$ and $\pi g_{7/2}$ orbitals contribute only very little to the wave functions. Also, such allowed M2 transitions usually show strengths below 1 W.u., in contrast to the collectively-enhanced E3 rates. Therefore, the retardation by a factor 10^{-3} is understandable.

Another interesting point is the striking similarity between the structure of ^{204}Tl states in the 18^+ to 22^- spin range with those from $45/2^-$ to $53/2^+$ recently established in ^{203}Hg [26]. One more, an $h_{11/2}$ proton, hole is present in ^{203}Hg and it gives rise to a sequence of high-spin states similar to ^{204}Tl , but with changed parity and spin values higher by 9/2 units. We shall demonstrate the observed analogy by recapitulating the observed structure and γ decay in the ^{204}Tl case and by providing the corresponding numbers for ^{203}Hg in brackets. The ^{204}Tl 22^- (^{203}Hg $53/2^+$) isomeric state decays preferentially by an M2 transition of 1542 keV (1320 keV) to the 20^+ ($49/2^-$) level. Two weaker competing branches proceed to two 19^+ ($47/2^-$) states via 954-(754) and 1085-(887) keV E3 transitions. It is remarkable that in all three cases the difference in transition energies is very close to 200 keV. This can be attributed to a -200 keV shift of the $53/2^+$ state in ^{203}Hg . Moreover, the γ decay of both 19^+ ($47/2^-$) states favors M1 transitions of 589-(566) and 458-(433) keV energies with respect to the 20^+ ($49/2^-$) state. This is a rare example of the yrast intensity flow from lower to higher spin happening in both nuclei. Also, a weaker M1 763-(694) keV branch from the lower-lying 19^+ ($47/2^-$) level to the 18^+ ($45/2^-$) states was detected in both cases. Moreover, the E2 decay from the 20^+ ($49/2^-$) level to the 18^+ ($45/2^-$) state by a 305-(261) keV transition is a feature observed in common. Finally, the inspection of the reduced transition probability values of Table III indicates that, for both nuclei, the 22^- ($53/2^+$) isomeric decay proceeds in a very similar way and with similar rates. The predominant M2 transitions have nearly identical $B(\text{M2})$ values with retardation factors of 0.93×10^{-3} (1.2×10^{-3}) and two weaker E3 branches have $B(\text{E3})$ values in the range of the single-particle estimate with 0.36 (0.9) and 0.44 (2.1) W.u., respectively. The higher $B(\text{E3})$ values extracted for both E3 transitions in ^{203}Hg could imply a stronger involvement of the octupole 3^- core excitation, but large uncertainties in these values (see Table III) do not allow to conclude firmly about such an effect.

It has to be emphasized that, in both ^{204}Tl and ^{203}Hg , calculations strongly favor the proposed spin-parity and intrinsic structures assigned to states from 18^+ ($45/2^-$) to 22^- ($53/2^+$). The calculations appear to be reliable in this region of low level density where the spin that can be reached from the valence particles is close to be exhausted.

TABLE III. Reduced transition probabilities for E3 and M2 transitions occurring in the decay of isomeric states in ^{204}Tl , ^{205}Tl and ^{203}Hg nuclei. Information listed in columns 2 to 6 was used to obtain the transition rates.

Isomeric state			Isomeric transition		$B(\text{E3})$			$B(\text{M2})$	
E (keV)	I^π	$T_{1/2}$ (μs)	E_γ (keV)	γ branch (%)	L^π	($10^3 e^2 \text{fm}^6$)	W.u.	($e\hbar/2\text{Mc}$) $^2 \text{fm}^2$	W.u. $\times 10^{-3}$
^{204}Tl									
1104.1	7^+	61.7 (10)	690.1	96.5	E3	0.255 (4)	0.103 (2)		
2319.0	12^-	2.6 (2)	668.9	96.2	E3	7.5 (6)	3.03 (24)		
4391.6	18^+	0.42 (3)	1036.3	61 (5)	E3	1.38 (15)	0.56 (6)		
			754.3	35 (4)	M2			0.175 (24)	3.0 (4)
6239.4	22^-	0.090 (3)	1542.4	80 (5)	M2			0.053 (4)	0.93 (7)
			1084.8	12 (2)	E3	0.89 (15)	0.36 (6)		
			954.1	5.8 (13)	E3	1.10 (25)	0.44 (10)		
^{205}Tl [14]									
3291	$25/2^+$	2.6 (2)	739	97	E3	3.77 (29)	1.51 (12)		
4836	$35/2^-$	0.235 (10)	1217	99	E3	1.30 (6)	0.522 (25)		
^{203}Hg [26]									
933	$13/2^+$	24 (4)	341.5	53	M2			0.24 (4)	4.3 (7)
8281	$53/2^+$	0.146 (30)	1320.3	78 (9)	M2			0.068 (16)	1.20 (28)
			887.4	12 (4)	E3	2.3 (9)	0.9 (4)		
			753.9	9(3)	E3	5.1 (22)	2.1 (9)		

E. Octupole core excitations and higher-lying states above the 22^- isomer

Above the 22^- isomeric state, a complex structure of ^{204}Tl levels was established in this work as seen in the level scheme of Fig. 5. The observed states must clearly involve particle-hole core excitations across the $N = 126$ and $Z = 82$ shell gaps. However, at present, no attempt was made to include configurations of this complexity in our shell model calculations. Consequently, the absence of support from calculations combined with a rather incomplete experimental input do not allow to propose firm spin-parity assignments and a possible interpretation of the observed states must remain rather restricted. Moreover, the presently established level scheme is incomplete. As pointed out earlier, a number of transitions from Table II could not be safely placed.

Nevertheless, a few spin-parity assignments are suggested, as indicated in Fig. 5. Apart from the 25^+ and 23^- states, which will be discussed below, all other assignments must be considered as tentative and based solely on arguments related to general characteristics of yrast γ decays. In fact, we assume that, above the 25^+ state, most transitions proceed with $\Delta I = 1$ spin changes, except for the competing cross-over transitions that are likely to be of E2 character. This fairly conservative approach was adopted to show that the yrast sequence of ^{204}Tl levels populated in the $^{48}\text{Ca} + ^{208}\text{Pb}$ deep-inelastic heavy-ion reaction can be observed up into the $I = 30$ spin range. It has to be noted that this high spin value does not represent a limit for the angular momentum that can be accessed in deep-inelastic

heavy-ion reaction spectroscopy. In the absence of any higher-lying isomer, the present analysis involved prompt γ transitions for which the complexity of the data limits the detection sensitivity. More weakly populated states, possibly of yet higher spin, might be observed in the future in instances where the existence of an appropriate isomer would increase the sensitivity of the analysis.

We now shall focus the discussion on two states located at the distinct yrast positions of 7052 and 8447 keV, both of which are distinguished by their predominant decay via high-energy 2207- and 2355-keV transitions to the 22^- and 20^+ final states, respectively. In particular, the strongly populated 8447-keV state, which collects the main intensity of yrast decay from higher-lying states, exhibits the features of a high-spin level located very favorably in excitation energy. An important, helpful observation is that both states apparently have lifetimes safely estimated to be longer than 2 ps, which favors a multipolarity higher than M1 or E2 for the associated de-excitations. This is concluded from the inspection of the shapes of the 2207- and 2355-keV intense γ lines which do not show any trace of Doppler broadening. In both cases, the summed intensity of feeding transitions is significantly lower than the decay intensity, indicating sizable direct state population. Consequently, from the absence of Doppler broadenings, it can be safely concluded that the decay out of both states is much slower than the stopping time of the ^{204}Tl product nuclei in a thick target.

We tentatively characterize both transitions as stretched E3 decays and assign spin and parity 25^+ and 23^- to the 8447- and 7052-keV states, respectively. For

the 7052-keV state, the observed competing 812-keV strong γ decay branch to the 22^- isomer is consistent with an M1 transition following from this assignment. The hindrance factor of the M1 transition is > 100 , consistent with a major change in structure. Both states are then proposed to arise from a stretched coupling of the 3^- octupole excitation of the ^{208}Pb core with the 22^- and 20^+ states with pure configurations $\pi h_{11/2}^{-1}\nu i_{13/2}^{-3}$ and $\pi h_{11/2} - 1\nu i_{13/2}^{-2} f_{5/2}^{-1}$. The observed features are identical to those observed in many other nuclei from the ^{208}Pb region, where such E3 excitations were identified and located immediately above states with valence particles or holes coupled to maximum spin values [3, 13], and requiring core excitations to form higher spin states. The remarkable validity of a simple additivity rule was established for a number of such states observed in experiments. It allows to calculate the energy of the observed E3 excitations built on states with complex structure from E3 energies established for the corresponding states with a simpler configuration. By simple addition of appropriate energy shifts from the initial 2615-keV energy of the ^{208}Pb 3^- excitation, the E3 energy observed for a more complex state can be reproduced surprisingly well. A number of examples demonstrating the validity of this rule was presented earlier for E3 excitations built on two particle (hole) states [3, 13]. Recently, a good case was presented for ^{205}Tl in which such a stretched E3 transition was located above the $35/2^-$ isomer arising from the coupling of two-neutron and one-proton holes. In this case, the experimental energy shifts known from E3 transitions observed in ^{207}Tl above the $11/2^-$ state and in ^{206}Pb above the 12^+ state gave a 2252-keV E3 energy for ^{205}Tl to be compared with the 2256-keV value observed in experiment [14].

For the 8447-keV state in ^{204}Tl , the coupling of an E3 excitation with the 22^- state of $\pi h_{11/2}^{-1}\nu i_{13/2}^{-3}$ structure involves the $\Delta E = -150$ keV shift known for the $h_{11/2}$ proton hole in ^{207}Tl and a shift arising from the interaction with three $i_{13/2}$ neutron holes coupled to maximum spin. Although the corresponding E3 transition above the $33/2^+$ ^{205}Pb isomer has not yet been identified experimentally, the expected energy shift can be estimated. The $\Delta E = -129$ keV shift known for the E3 excitation above the $i_{13/2}$ hole state in ^{207}Pb [29] and the $\Delta E = -212$ keV shift observed for the E3 excitation above the 12^+ , $i_{13/2}^{-2}$ state allow to attribute a smaller shift of $\Delta E = -83$ keV arising from the second $i_{13/2}$ neutron hole. This gives an estimate of $\Delta E = -262$ keV for the total shift for a $i_{13/2}^{-3}$, $33/2^+$ state by applying a similar reduction factor for a shift attributed to the third $i_{13/2}$ neutron hole. Summing up the shifts arising from all four holes, one obtains the $\Delta E = -412$ keV total energy shift which gives a 2203-keV E3 transition energy, in excellent agreement with the 2207-keV value observed in the experiment.

A similar procedure can be applied to the 7052-keV state, which is interpreted as the 3^- core excitation built

on the 20^+ state of pure $\pi h_{11/2}^{-1}\nu i_{13/2}^{-2} f_{5/2}^{-1}$ configuration. Here, all required shifts are known from experiment with $\Delta E = -150$ keV for $\pi h_{11/2}^{-1}$, $\Delta E = -212$ keV for $\pi i_{13/2}^{-2}$, and the previously established [30] $\Delta E = +41$ keV for the stretched E3 excitation built on the $f_{5/2}$ neutron hole. The resulting 2294-keV E3 transition energy is lower by 61 keV than the experimentally observed value of 2355 keV. Nevertheless, it is much higher than the 2207-keV energy observed for the 25^+ state, in agreement with the repulsive interaction established for the stretched E3 coupling with the $f_{5/2}$ neutron hole present in the 20^+ state structure.

V. SUMMARY AND CONCLUSIONS

The high-spin structure of the neutron-rich ^{204}Tl isotope has been studied up to an excitation energy of 11.2 MeV and a $I = 30$ spin range using the deep-inelastic heavy-ion γ spectroscopy method. The high-quality γ coincidence data from experiments using the Gammasphere array combined with the complex analysis involving the selective use of timing parameters allowed to reveal fairly complete spectroscopic information in this hitherto poorly studied and hard-to-access Tl isotope. A readily understood structure of yrast levels, including four isomeric states, was established and interpreted up to the 22^- , highest-spin state available for maximally-aligned three neutron- and one proton- valence holes. The performed up-to-date shell model calculations result in an excellent agreement with the experimentally observed levels and served as a guide for unique spin-parity assignments, otherwise largely based on experimental input. The structure of the observed levels was extensively discussed also based in part on considerations of observed γ decays, with a particular emphasis placed on the M2 and E3 decays of isomeric states. A striking analogy of the structure of levels between the 18^+ and 22^- isomers in ^{204}Tl with the recently identified corresponding states in ^{203}Hg was demonstrated. The rather general discussion of the structure of high-spin states located above the 22^- isomer was followed by a detailed examination of two prominently populated states likely arising from the stretched coupling of the 3^- first excited, octupole state of the ^{208}Pb core with the highest-spin states available for four valence holes of ^{204}Tl . The applicability of the empirical rule proposed earlier to estimate energies of such states was demonstrated.

ACKNOWLEDGMENTS

This work was supported by the US Department of Energy, Office of Nuclear Physics, under contract No DE-AC-02-06CH11357 and by the Polish Ministry of Science and Higher Education Grant No 1P03B05929.

-
- [1] L. Rydström, J. Blomqvist, R. J. Liotta, C. Pomar, Nucl. Phys. A **512**, 217 (1990).
- [2] K. H. Maier *et al.*, Phys. Rev. C **76**, 064304 (2007).
- [3] R. Broda, J. Phys. G **32**, R151 (2006).
- [4] M. Rejmund *et al.*, Z. Phys. A **359**, 243 (1997).
- [5] G. J. Lane *et al.*, Phys. Lett. B **606**, 34 (2005).
- [6] B. Fornal *et al.*, Phys. Rev. C **67**, 034318 (2003).
- [7] R. Broda *et al.*, Eur. Phys. J. A **20**, 145 (2004).
- [8] B. Fornal *et al.*, Phys. Rev. Lett. **87**, 212501 (2001).
- [9] S. J. Steer *et al.*, Phys. Rev. C **78**, 061302(R) (2008).
- [10] Evaluated by F. G. Kondev and S. Lalkovski, Nuclear Data Sheets **112**, 707 (2011).
- [11] Evaluated by F. G. Kondev, Nuclear Data Sheets **109**, 1527 (2008).
- [12] M. Rejmund, Ph.D. Thesis GSI DISS 99 03 (1999).
- [13] M. Rejmund *et al.*, Eur. Phys. J. A **8**, 161 (2000).
- [14] J. Wrzesiński *et al.*, Eur. Phys. J. A **20**, 57 (2004).
- [15] Evaluated by C. J. Chiara and F. G. Kondev, Nuclear Data Sheets **111**, 141 (2010).
- [16] K. H. Maier, Nucl. Phys. A **195**, 577 (1972).
- [17] M. Pfuetzner *et al.*, Phys. Lett. B **444**, 32 (1998).
- [18] R. Broda *et al.*, Phys. Lett. B **251**, 245 (1990).
- [19] N. Fotiades, R. O. Nelson, M. Devlin, J. A. Becker, Phys. Rev. C **77**, 024306 (2008).
- [20] I. Y. Lee, Nucl. Phys. A **520**, 641c (1990).
- [21] C.G. Linden, I. Bergstrom, J. Blomqvist, K.-G. Rensfelt, H. Sergolle, K. Westerberg, Z. Phys. A **277**, 273 (1976).
- [22] N. Roy, K.H. Maier, A. Aprahamian, J.A. Becker, D.J. Decman, E.A. Henry, L.G. Mann, R.A. Meyer, W. Stoeffl and G.L. Struble, Phys. Lett. B **221**, 6 (1989).
- [23] B. A. Brown, A. Etchegoyen, N. S. Godwin, W. D. M. Rae, W. A. Richter, W. E. Ormand, E. K. Warburton, J. S. Winfield, L. Zhao and C. H. Zimmerman, MSU-NSCL Report No. 1289 (2004).
- [24] G. Audi, A. H. Wapstra, C. Thibault, Nucl. Phys. A **729**, 337 (2003).
- [25] J. B. McGrory, T. T. S. Kuo, Nucl. Phys. A **247**, 283 (1975).
- [26] B. Szpak *et al.*, Phys. Rev. C **83**, 064315 (2011).
- [27] N. Frascaria, J. P. Didelez, N. S. Chant and C. C. Chang, Phys. Rev. C **16**, 603 (1977).
- [28] P. A. Smith, R. J. Peterson, R. A. Emigh and R. E. Anderson, Nucl. Phys. A **342**, 437 (1980).
- [29] M. Schramm *et al.*, Z. Phys. A **344**, 121 (1992).
- [30] M. Kadi, P. E. Garrett, Minfang Yeh, S. W. Yates, T. Belgya, A. M. Oros-Peusquens, K. Heyde, Phys. Rev. C **61**, 034307 (2000).